

# **On the Increase of Background Seismicity Rate during the 1997-1998 Umbria-Marche, Central Italy, Sequence: Apparent Variation or Fluid-Driven Triggering?**

**Anna Maria Lombardi, Massimo Cocco and Warner Marzocchi**

**Istituto Nazionale di Geofisica e Vulcanologia, Via di Vigna Murata 605, 00143 Rome, Italy.**

Submitted to BSSA

2009

## Abstract

We investigate the temporal evolution of background seismicity rate in the Umbria-Marche sector of the northern Apennines that was struck by the 1997-98 Colfiorito seismic sequence. Specifically we apply the ETAS model to separate the background seismicity rate from the coseismic triggered rate of earthquake production. Analyzed data are extracted from the CSI1.1 catalog of Italian seismicity (1981-2002), which contains for the study area 12.163 events with  $M_L > 1.5$ . The capability of the ETAS model to match the observed seismicity rate is tested by analyzing the model residuals and by applying two non-parametric statistical tests (the RUNS and the Kolmogorov-Smirnov tests) to verify the fit of residuals to Poisson hypothesis. We first apply the ETAS model to the seismicity occurred in the study area during the whole period covered by the CSI1.1 catalog. Our results show that the ETAS model does not explain the temporal evolution of seismicity in a time interval defined by change points identified from time-evolution of residuals and encompassing the Colfiorito seismic sequence. We therefore restrict our analysis to this period and analyze only those events belonging to the 1997-1998 seismic sequence. We again obtain the inadequacy of a stationary ETAS model with constant background rate to reproduce the temporal pattern of observed seismicity. We verify that the failure of ETAS model to fit the observed data is caused by the increase of the background seismicity rate associated with the repeated Colfiorito main shocks. We interpret the inferred increase of background rate as a consequence of the perturbation to the coseismic stress field caused by fluid flow and/or pore pressure relaxation. In particular we show that the transient perturbation caused by poroelastic relaxation can explain the temporal increase of background rate that therefore represents a fluid signal in the seismicity pattern.

## Introduction

It is widely accepted that short-term clustering of seismicity is promoted by stress perturbations caused by earthquake ruptures [Stein, 1999; King and Cocco, 2000; Steacy *et al.*, 2005 and references therein]. Several physics-based models have been proposed to simulate the rate of earthquake production [Dieterich, 1992, 1994; Gomberg *et al.*, 2005 and references therein]; some of them have been also applied to forecast seismicity rate changes [Toda and Stein, 2003; Toda *et al.*, 2005; among several others]. Despite their current and widespread application, a robust validation of the forecasting capabilities has not been performed and their application to society is still not fully demonstrated [Woessner *et al.*, 2009]. From a phenomenological point of view, the seismicity rate  $\lambda(t)$  of aftershock sequences generally decays according to the modified Omori law

$$\lambda(t) = \frac{k}{(t + c)^p} \quad (1)$$

where  $t$  is the elapsed time since the mainshock and  $k$ ,  $c$  and  $p$  are constants [Utsu *et al.*, 1995], which might be spatially non-uniform [Wiemer and Wyss, 2002; Gerstenberger *et al.*, 2005; Hainzl *et al.*, 2009].

A well-established statistical tool to analyze the spatial and temporal patterns of shallow seismicity is the Epidemic-Type Aftershock Sequences (ETAS) model [Ogata, 1988; 1998]. This approach describes the seismicity pattern in time and space in agreement with the modified Omori and the Gutenberg-Richter laws taking into account the possibility of secondary triggering of aftershocks. The ETAS model has been widely adopted in the literature [Helmstetter and Sornette, 2002; 2003; Console *et al.*, 2003; Zhuang *et al.*, 2004; Ogata and Zhuang, 2006, among many others] to measure the background seismicity rate and the clustered triggered seismicity. The common interpretation of ETAS modeling results relies on associating the latter with the coseismic stress changes caused by earthquakes occurred within the study area [Ogata, 2005a; 2005b; 2006]. The background seismicity rate is frequently modeled as spatially non-uniform but stationary in time, although non-stationary ETAS or more sophisticated stochastic models have been proposed to capture temporal fluctuations at different time scales in the rate of earthquake production [Hainzl and Ogata, 2005; Lombardi *et al.*, 2006; Lombardi and Marzocchi, 2007; Marzocchi and Lombardi 2008.].

Coseismic stress perturbations are commonly represented through Coulomb stress changes [King *et. al.*, 1994; Harris, 1998; King and Cocco, 2000]. In the literature, most of the applications rely on the computation of static stress changes, although the role of dynamic stress perturbations in earthquake triggering is widely debated [see Kilb *et al.*, 2000; Gomberg and Jonhson, 2005, and references therein]. However, it is well known that coseismic stress changes can be further

modified by other processes such as viscoelastic relaxation [Pollitz, 1992; Piersanti *et al.*, 1995; Freed, 2005], pore pressure relaxation and fluid flow [Nur and Booker, 1972; Miller *et al.*, 2004; Manga and Wang, 2007] or aseismic slip and afterslip [Marone *et al.*, 1991; Wennerberg and Sharp, 1997; Pollitz *et al.*, 1998; Helmstetter and Shaw, 2009]. Whereas the viscoelastic relaxation can contribute to stress perturbations over long time scales, pore pressure relaxation, fluid flow and afterslip can play a dominant role in triggering seismicity at time scales compatible with aftershocks duration [Nur and Booker, 1972; Marone *et al.*, 1991; Wennerberg and Sharp, 1997; Miller *et al.*, 2004; Antonioli *et al.*, 2005].

Several recent papers proposed to use the ETAS model as an appropriate tool also to identify the effects of transient perturbations to the tectonic remote loading rate and, therefore, to extract the signal of aseismic slip, afterslip or fluid driven triggering of seismicity [Hainzl and Ogata, 2005; Lombardi *et al.*, 2006; Llenos *et al.*, 2009 and references therein]. To this goal, the analysis of the background rate is of particular importance; indeed, while a stationary background is usually explained in terms of a nearly constant tectonic loading rate, a temporal variation of the background rate can point out the presence of other physical processes (viscoelastic relaxation, fluid flow or afterslip) affecting the rate of earthquake production [Hainzl and Ogata, 2005; Lombardi *et al.*, 2006; Lombardi and Marzocchi, 2007; Marzocchi and Lombardi, 2008; Llenos *et al.*, 2009].

In this paper, we deal with this issue and we aim to study the complex Umbria-Marche seismic sequence [Chiaraluce *et al.*, 2003 and 2004, and references therein; Marzocchi, 2008] occurred in 1997-1998 in the northern Apennines (Central Italy). The presence of fluids in this area has been recognized by previous studies [Chiodini *et al.*, 2000]. The role of pore pressure relaxation and/or fluid flow, promoted by elastic stress changes caused by the largest magnitude main shocks, has been investigated to model the evident migration of seismicity during the sequence [Chiaraluce *et al.*, 2003; Miller *et al.*, 2004; Antonioli *et al.*, 2005]. Moreover, post-seismic deformation following the Umbria-Marche main shocks has been observed through GPS measurements and modeled by viscoelastic relaxation and afterslip [Riva *et al.*, 2007]. In the present study, we apply the ETAS model in order to demonstrate that during the sequence there was an increase of the background seismicity rate and we interpret our results in terms of fluid-driven earthquake triggering.

## The study area

We select a study area comprising the sector of the Northern Apennines (Central Italy) struck by Umbria-Marche seismic sequence in 1997-1998 (see Figure 1). In this study, we use the seismic catalog "Catalogo della Sismicità Italiana (CSI1.1) 1981–2002" [Castello *et al.*, 2005,

2007], which contains the shallow seismicity (depth  $\leq$  30km) occurred in Italy from January 1<sup>st</sup> 1981 to December 31<sup>st</sup> 2002 and we extract from it a data set containing the seismicity occurred in the study area. The selected dataset contains 12.163 seismic events with magnitude  $M_L \geq 1.5$  and includes 9 events with magnitude  $5.0 \leq M_L \leq 6.0$ , 8 of which belong to 1997-1998 Umbria-Marche sequence. Figure 1 shows the epicenters of the selected earthquakes and the focal mechanisms of the largest shocks.

The 1997 Umbria-Marche seismic sequence consists of thousands of events that in few tens of days activated a NW-trending normal fault system [*ChiaraLuce et al.*, 2003, 2004 and references therein]. The sequence is characterized by a clear migration of seismicity from NW to SE with the progressive activation of adjacent fault segments [see *Antonioli et al.*, 2005]. The two largest earthquakes of the sequence ( $M_L=5.6$  and  $M_L=5.8$ ) struck the Colfiorito area on September 26<sup>th</sup> 1997 within 9 hours and few kilometers of distance from each other. They were followed by two other main shocks with similar magnitude ( $M_L=5.0$  and  $M_L=5.4$ ) at the beginning of October (the 3<sup>rd</sup> and 6<sup>th</sup> of October). Then, the seismicity began to migrate towards SE, where two other main shocks with magnitude larger than 5.0 occurred in the Sellano area on October 12<sup>th</sup> ( $M_L 5.1$ ) and October 14<sup>th</sup> ( $M_L 5.5$ ). Finally, other two main shocks ( $M_L=5.4$  and  $M_L=5.3$ ) occurred in the area near Gualdo Tadino, north of Colfiorito, few months later in 1998 (March 28<sup>th</sup> and April 3<sup>rd</sup>), the former is a sub-crustal deep earthquake. A comprehensive description of this seismic sequence can be found in *ChiaraLuce et al.* [2003, 2004].

A correct understanding of the physical processes controlling the rate of earthquake production depends on the accuracy and homogeneity of the available seismic catalog. Specifically, a critical issue, that has to be addressed before performing any investigation, is the assessment of quality and homogeneity of magnitudes [*Zuniga and Wiemer*, 1999]. Changes in monitoring capabilities (that is, introduction of new hardware or software in the network, removal or addition of seismic stations, changes in magnitude definition) are often misinterpreted as real seismicity anomalies. However, the earthquake parameters of the CSI1.1 catalog have been revised by *Castello et al.* [2007], thus in our study the magnitude scale can be considered homogeneous in time. Here we verify the completeness magnitude ( $M_c$ ) and its variations with time.  $M_c$  is defined as the lowest magnitude at which 100% of the events are detected. Below  $M_c$ , the catalog does not contain a fraction of expected seismic events, because they are too small to be recorded by a sufficient number of recording stations or, in the case of aftershock sequences, because they are too small to be detected by the network. *Woessner and Wiemer* [2005] compare different methods for estimating  $M_c$  from instrumental catalogs, all assuming the self-similarity of the earthquake process. They show that the Maximum Curvature (MAXC) Method [*Wiemer and Wyss*, 2000] is a fast

procedure that provides a reasonable estimate of  $M_c$ , also in case of small datasets. Moreover, they propose a bootstrap method to estimate the uncertainty of  $M_c$  measure. The algorithms are freely available together with the software package ZMAP [Wiemer, 2001]. The analysis of our whole catalog by MAXC method provides a value of  $M_c$  equal to 1.7 (see Figure 2a), but the analysis of the temporal variation of completeness magnitude shows clear changes of  $M_c$  with time (see Figure 2b). In particular,  $M_c$  decreases from 2.3 to about 1.6 in time. The  $M_c$  peaks near the end of 1997 ( $M_c=2.3$ ) corresponds to the beginning of the 1997-1998 Umbria-Marche seismic sequence: it reveals a decrease of aftershocks detection for  $M < M_c$  immediately after the occurrence of the two September 26<sup>th</sup> main shocks. Since the MAXC Method underestimates  $M_c$  on average by 0.2 [Woessner and Wiemer, 2005], we have selected for our analysis only the events with magnitude larger than 2.5 (1.586 events). This choice guarantees the achievement of a complete and homogenous dataset for the whole time period covered by CSI1.1 catalog.

## The Spatio-Temporal Epidemic Type Aftershock Sequences (ETAS) Model

The Epidemic-Type Aftershocks Sequences (ETAS) Model is a stochastic point process describing clustered seismicity and, therefore, it is of particular relevance for stress-triggered aftershock sequences. Since the first time-magnitude formulation proposed by Ogata [1988], many others time-magnitude-space versions have been published in the literature, mostly based on empirical studies of past seismicity [Ogata, 1998; Console et al., 2003; Zhuang et al., 2002]. These approaches describe the seismicity rate of a specific area as the sum of two contributions: the "*background rate*", which refers to seismicity not triggered by precursory events present in any catalog and usually associated with the regional tectonic strain rate, and the "*rate of triggered events*" associated with stress perturbations caused by previous earthquakes. The main feature of ETAS model is that each earthquake has some magnitude-dependent ability to perturb the rate of earthquake production and therefore to generate its own Omori-like aftershock decay.

The last improved extension of ETAS model, proposed by Ogata and Zhuang [2006], defines the total space-time conditional intensity  $\lambda(t,x,y/\mathcal{H}_t)$  (i.e. the probability of an earthquake occurring in the infinitesimal space-time volume conditioned to all past history) by equation:

$$\lambda(t,x,y/\mathcal{H}_t) = vu(x,y) + \sum_{t_i < t} \frac{K}{(t - t_i + c)^p} e^{\alpha(M_i - M_c)} \frac{c_{d_{q\gamma}}^i}{[r_i^2 + (de^{\gamma(M_i - M_c)})^2]^q} \quad (2)$$

where  $\mathcal{H}_t = \{(t_i, x_i, y_i, M_i); t_i < t\}$  is the observation history up to time  $t$ ,  $M_c$  is the completeness magnitude of the catalog,  $u(x, y)$  is the spatial probability density function (PDF) of background events,  $c_{d, q, \gamma}^i = \frac{q - 1}{\pi} \int (de^{\gamma(M_i - M_c)})^2 \int^{q-1}$  is the normalization constant of the spatial PDF for triggered events, and  $r_i$  is the distance between location  $(x, y)$  and the epicenter of  $i$ -th event  $(x_i, y_i)$ . This version of the ETAS model is characterized by the introduction of the term  $e^{\gamma(M_i - M_c)}$  that takes into account the correlation between the aftershocks area and the mainshock magnitude, in agreement with the relation proposed by *Utsu and Seki* [1955].

The parameters  $(v, K, c, p, \alpha, d, q, \gamma)$  of the model, for the events occurred within a time interval  $[T_1, T_2]$  and a region  $R$ , can be estimated by maximizing the Log-Likelihood function [*Daley and Vere-Jones*, 2003], given by

$$\log L(v, K, c, p, \alpha, d, q, \gamma) = \sum_{i=1}^N \log \lambda(t_i, x_i, y_i / H_{t_i}) - \int_{T_1}^{T_2} \int_R \lambda(t, x, y / H_t) dt dx dy. \quad (3)$$

Specifically, to estimate the parameters for our dataset, we apply the iteration algorithm developed by *Zhuang et al.* [2002]. By using a suitable kernel method, this procedure provides, in addition to the model parameters, also an estimation of the PDF  $u(x, y)$  for background events.

Because several physical investigations show that static stress changes decrease with epicentral distance as  $r^{-3}$  [*Hill et al.*, 1993; *Antonioli et al.*, 2004], in the present study we impose  $q=1.5$ . This choice is also justified by the recognized trade-off between parameters  $q$  and  $d$  that may cause different pairs of  $q$  and  $d$  values to provide almost the same likelihood of the model [*Kagan and Jackson*, 2000].

The analysis of model residuals [*Ogata*, 1988] can be used to test the correctness of the ETAS model. These are obtained by transforming occurrence times  $t_i$  into new values  $\tau_i$  using the relation

$$\tau_i = \int_{T_{start}}^{t_i} dt \int_R dx dy \lambda(t, x, y / H_t) \quad (4)$$

where  $T_{start}$  is the starting time of the observation history. It is well known that, if the ETAS describes the temporal evolution of seismicity, the transformed data  $\tau_i$  are expected to behave like a stationary Poisson process with the unit rate [*Ogata*, 1988], i.e. the values  $\Delta\tau_i = \tau_{i+1} - \tau_i$  are independent and exponentially distributed (with mean equal to 1) random variables. We check this hypothesis by means of two nonparametric tests: the Runs test, to verify the reliability of the independence property, and the one-sample Kolmogorov-Smirnov (KS1) test, to check the standard exponential distribution [*Gibbons and Chakraborti*, 2003; *Lombardi and Marzocchi*, 2007]. We use

both tests because all goodness-of-fit tests (as KS1) are ineffective to check the presence of a memory in the time series. Hence, any discrepancy of residuals by Poisson hypothesis identified by just one or both tests is a sign of inadequacy of ETAS model to explain all basic features of analyzed seismicity.

## Application of the ETAS model to the 1981-2002 Umbria-Marche seismicity

In order to investigate the seismicity pattern and the clustering of earthquakes in the Umbria-Marche region (see Figure 1), we apply the ETAS model to a dataset containing all seismic events in the study area included in the CSI1.1 catalog. Following the procedure described in the previous section, we estimate the model parameters from the seismic catalog. Table 1 lists the inferred values of model parameters together with their errors and the associated log-likelihood values. The retrieved values of  $p$  and  $a$  parameters are similar to those obtained by previous studies in other tectonic areas [Ogata, 1992]. The estimated value of the parameter  $\gamma$  suggests that the dependence on magnitude of distance  $d$  is rather weak; in other words, the scaling of aftershock area against the magnitude of the causative event is weak, although not totally negligible. According to the ETAS model, we can compute the probability  $\rho_i$  that the  $i$ -th event belongs to background seismicity and the probability  $\sigma_{ij}$  that it is triggered by a previous  $j$ -th event. They are given by

$$\rho_i = \frac{v u(x_i, y_i)}{\lambda(t_i, x_i, y_i / H_{t_i})} \quad (5)$$

$$\sigma_{ij} = \frac{K e^{\alpha(M_j - M_{min})} (t_j - t_i + c)^{-p} c_{dq\gamma} \left[ r_{ij}^2 + (d e^{\gamma(M_j - M_{min})})^2 \right]^{-q}}{\lambda(t_i, x_i, y_i / H_{t_i})}$$

All events with magnitudes larger than 5.0 belonging to 1997-1998 sequence have a probability larger than 90% to be triggered events. In particular, the first Colfiorito main shock of September 26<sup>th</sup> has a probability of solely 2% to be a background event. It is likely triggered by a foreshock with magnitude  $M_L = 4.4$ , occurred nearby on September 3<sup>rd</sup>, which can be considered as the initiation of seismic sequence.

In order to test the goodness of the inferred ETAS model, we analyze the residual as described in the previous section. The results of this test are shown in Figure 3a, which displays the cumulative number of residuals [ $N(\tau_i)$ ] as a function of the transformed times ( $\tau_i$ , as defined in 4). The expected Poissonian distribution of residuals should produce a linear scaling in the plot of Figure 3a (that is, the cumulative number of residuals should lie along the bisector). Any deviation

from this scaling is interpreted as a failure of the model to match the observed data. By using the Kolmogorov-Smirnov test (KS1) we cannot reject the null hypothesis that values  $\Delta\tau_i = \tau_{i+1} - \tau_i$  are exponentially distributed with mean equal to 1 (the significance level found is 0.4). On the other hand, the Runs test rejects the independence hypothesis of  $\Delta\tau_i$  (the significance level is equal to  $8 \cdot 10^{-4}$ ), implying that residuals are correlated, therefore they are not distributed according to a Poisson distribution. The plot reported in Figure 3a shows that several marked change points characterize the time evolution of the residuals. We find them by using the algorithm developed by *Mulargia and Tinti* [1985]. Specifically, we identify two significant change points at May 3<sup>rd</sup> 1997 and October 15<sup>th</sup> 1997 (see Figure 3a), which mark periods with different slope of the residuals.

In order to further investigate sudden temporal changes of seismicity, we check also the appropriateness of the stationary Poisson hypothesis for the background seismicity. A direct way to discuss how the background rate changes with time is to calculate the cumulative background seismicity defined by [Zhuang *et al.*, 2005]

$$S(t) = \sum_{t_i < t} \rho_i \quad (6)$$

Also in this case we reject null hypothesis by RUNS test (the significance level is  $1 \cdot 10^{-5}$ ). By applying the change point analysis also at this new variable, we identify three significant change points at May 3<sup>rd</sup> 1997, October 21<sup>st</sup> 1997 and August 17<sup>th</sup> 1998 (Figure 3b), highlighting a time period with a much higher background rate. The detection of change points is quite stable also analyzing the seismicity above  $M_c=3.0$ .

These results show that the ETAS model does not fully explain the temporal evolution of seismicity in the study area. The inferred change points suggest that the unfitness of the ETAS model occurs in a time window containing the Colfiorito seismic sequence. To better understand the causes of these inefficiencies, we select a subset of our catalog solely including the 1997-1998 seismic sequence. Considering previous results obtained with ETAS calculations, we select the seismicity occurred between May 3<sup>rd</sup> 1997, and August 17<sup>th</sup> 1998 (874 events).

## **Analysis of the 1997-1998 Colfiorito aftershocks sequence**

The discrepancy between model and data discussed in the previous section suggests the existence of some change in seismicity not captured by the estimated ETAS model. It is well known that the ETAS model parameters depend on the driving physical processes controlling the rate of earthquake production of the investigated region. In particular, the background rate  $\nu$  accounts for the non-coseismically triggered seismicity (i.e., which does not participate to the Omori decay) and it is controlled by the active tectonic loading rate including its transient perturbations (such as fluid

flow or aseismic processes) [Hainzl and Ogata, 2005; Lombardi et al., 2006; Catalli et al. 2008; Llenos et al., 2009]. The parameter  $p$  of the Omori law, controlling the temporal decay of triggered events, has been related to heat flow, the degree of structural heterogeneity (i.e., damage) in the fault zone as well as stress and crustal temperature [Mogi, 1967; Kisslinger and Jones, 1991; Utsu et al., 1995]. Moreover, swarm-like seismic activity has usually a smaller  $\alpha$ -value than the typical mainshock-aftershock sequences [Utsu et al., 1995]. Thus, we apply the ETAS model only to those events belonging to the Colfiorito aftershock sequence (that is, from May 3<sup>rd</sup> 1997 to August 17<sup>th</sup> 1998; named CAS, hereinafter) in order to get new insights on the physical processes affecting the seismicity. We emphasize that fixing the beginning of the sequence on May 3<sup>rd</sup> 1997 is consistent with results of the ETAS model applied to both the whole catalog and the background seismicity (Figure 3). The choice to select August 17<sup>th</sup> 1998 as the conclusion of the sequence is consistent with the analysis of background seismicity and with the inspection of the rate of earthquake production.

The results of these calculations are listed in Table 2. The comparison between these parameters with those estimated for the entire catalog covering the study area (listed in Table 1) does not reveal significant variations except for background rate  $v$ , which increases from  $0.055\pm0.003$  to  $0.13\pm0.02$   $day^{-1}$  reaching  $2.2\pm0.4$   $day^{-1}$  in the first month after the two Colfiorito mainshocks (September 26<sup>th</sup> - October 26<sup>th</sup> 1997). The respective values of background rate  $v$  for events with magnitude larger than  $M_c = 3.0$  are  $0.017\pm0.002$   $day^{-1}$  (whole catalog: January 1<sup>st</sup> 1981- December 31<sup>st</sup> 2002),  $0.04\pm0.01$   $day^{-1}$  (for the CAS) and  $0.8\pm0.3$   $day^{-1}$  (September 26<sup>th</sup> - October 26<sup>th</sup> 1997). No relevant variation of the other parameters has been found for  $M_c = 3.0$ . By applying KS1 and RUNS tests on residuals  $\tau_i$  of events belonging to CAS with magnitudes larger than  $M_c = 2.5$ , we find that the Poisson hypothesis is rejected by KS1 test (significance level of  $5 \cdot 10^{-4}$ ). Moreover the change point analysis reveals two significant change points for distribution of residuals on Sept 26<sup>th</sup> 1997 and Oct 14<sup>th</sup> 1997. This result further confirms that the ETAS model does not match the observed data. It also indicates that the inferred increase of background rate during CAS is independent of the magnitude threshold  $M_c$  and this is the only significant change compared with the seismicity in the whole catalog for the study area.

To further investigate the significance of the detected increase of background seismicity rate, we have compared the observed and expected number of events per day during the sequence. (see Figure 4). Using the model parameters estimated for CAS period (see Table 2) we have obtained a general agreement between the predicted and the observed number of earthquakes. However, few discrepancies still remain (see also Marzocchi, 2008), especially in the earlier phase of the sequence, coinciding with the time period bounded by change points of residuals (Sept 26<sup>th</sup>-

Oct 14<sup>th</sup>). These discrepancies persist also when a minimum magnitude  $M_c = 3.0$  is used (see Figure 4b), and they could arise from inadequacy of an ETAS model to describe a sudden and sharp increase of the rate of earthquake production. At the same time, these results corroborate the significance of the estimated increase in the background seismicity rate  $v$  (equal to  $2.2 \text{ day}^{-1}$  for  $M_c=2.5$ ) in the first month of the sequence and suggest the need to take into account its variation in time and space during the CAS to fully describe the complex spatio-temporal evolution of the sequence. For these calculations, we have implemented the strategy outlined in *Lombardi et al.* (2006) to model the temporal variation of the background rate for the 2000 Izu seismic sequence. In the present study, we have also introduced the variation in time of the spatial distribution of background seismicity. This improvement is necessary to take into account the spatial, besides the temporal, evolution of the physical processes modifying the background rate. Essentially, the background of ETAS model ( $v(t) u(t,x,y)$ ) is recalculated for each time interval  $\tau$  of 5 and 10 days, where all the other parameters are taken equal to the values inferred for the whole sequence (see Table 2). In this way, we have a non-stationary ETAS model with the background varying in space and time. We show in Figure 5 the temporal evolution of the cumulative value of background seismicity inferred for the whole study area ( $v(t)$ ). Remarkably, the plot shows that the background seismicity experienced a marked increase at the end of September 1997 (when the two Sept. 26<sup>th</sup> main shocks occurred). The increase of background rate continued simultaneously to the occurrence of the largest magnitude shocks and, after the last main shock of October 14<sup>th</sup> 1997 near Sellano, it began to decrease back to the stationary state.

In order to check the statistical significance of the inferred non-stationary behavior of background rate, we have applied the corrected Akaike Information Criterion (AICc) [*Hurvich and Tsai, 1989*] to stationary and non-stationary ETAS models. The AICc methodology attempts to find the model that best explains the data with a minimum of free parameters. For the stationary ETAS model we have  $\text{AICc} = 7795.9$ . For two versions of non-stationary ETAS model, corresponding to different choices of  $\tau$ , we obtain  $\text{AICc} = 7794.6$  (for  $\tau$  equal to 5 days) and  $\text{AICc} = 7769.0$  (for  $\tau$  equal to 10 days). Keeping in mind that the best model has the lower value of AICc, these results indicate that the non-stationary ETAS model with  $\tau=10$  days is the best one to describe the data and it is significantly better than the stationary ETAS model. On the other hand, the non-stationary ETAS model with  $\tau=5$  days does not improve significantly the description of seismicity, probably due to overfitting of data (i.e. a too large number of parameters) after the last change point (Oct 31<sup>st</sup>, see Figure 5), when no significant variation of background is noticeable.

It is worthy of note that the nonstationary ETAS model with  $\tau=10$  days cannot be rejected by applying both Runs and KS1 tests on residuals, if the spatial and temporal variation of

background rate during this period is included into the modeling (the significance level of KS1 and Runs tests are 0.14 and 0.4, respectively). Taking into account all these results, the background variation represents a key contribution to significantly improve the goodness of ETAS fit to the observed rate of earthquake production during this sequence. Remarkably, by applying a time-dependent estimation of the other key parameters of the ETAS model we do not find any significant variation that can be identified by change points analysis.

## Interpretations

All previous results show that the stationary ETAS model (with a constant background rate) cannot be used to reveal the basic features of the Colfiorito aftershock sequence, and that the discrepancies between observations and ETAS predictions occur in a time interval encompassing the aftershock sequence. The most likely cause of this inadequacy appears to be a strong underestimation of the real background rate during the most productive initial phase of the sequence. We identify two main potential factors explaining this finding: (1) a transient temporal variation of the external loading rate caused by physical processes complementary to the regional tectonic stressing rate and to the coseismic stress perturbations, and/or (2) a bias into the background rate estimation, that could cause an apparent increase of non-coseismically-triggered seismicity. As regard to this latter issue, it has been proposed that earthquake triggering is mostly controlled by the smallest magnitudes [Felzer *et al.*, 2003; Helmstetter *et al.*, 2005]. The undetected seismicity below the minimum magnitude  $M_c$  might affect the background rate variations, causing a consequent significant overestimation of background rate [Sornette and Werner, 2005]. Therefore, the sudden increase of overall seismicity during the CAS could have led to the observed increase of the background seismicity rate.

In order to better understand this issue we analyze numerically two classes of 1000 simulated synthetic catalogs. The catalogs of the first class contain the real observed seismicity until September 26<sup>th</sup>, in order to include the initial phase of real sequence; afterward, the catalogs contain simulated events generated by the ETAS model with the parameters reported in Table 2 and a minimum magnitude equal to 2.5. At each simulated event we assign the real sequence of magnitudes reported by the real catalog. In summary, this class of catalogs contains only a random sequence of aftershocks in terms of time of occurrence and location. Each synthetic catalog ends when the number of events reaches that of the original catalog. The synthetic catalogs of the second-class have the same duration of the original whole CSI1.1 catalog (Jan 1<sup>st</sup> 1981- Dec 31<sup>th</sup> 2002), but have a minimum magnitude equal to 1.0. The magnitudes of events are simulated in agreement with the Gutenberg-Richter law; the used b-value, equal to 0.99, is estimated by using

the maximum likelihood method on the whole Umbria-Marche catalog. The analysis of such synthetic datasets has two rationales: 1) to check if the amplitude of the background rate variation observed for real seismicity can be explained by chance; 2) to check if the background rate increase can be due to the triggering effects of events smaller than the minimum adopted magnitude ( $M_c=2.5$ ) which are not included in our calculations. The simulations are performed by the thinning method proposed by *Ogata* [1998].

The duration of simulated catalogs belonging to the first class is on average about 3 years longer than the Umbria-Marche sequence. This means that the synthetic catalogs generated by ETAS model with the parameters reported in Table 2 yield a significant underestimation of the real seismicity rate. Notably, simulated seismicity rates for the first class of synthetic catalogs also underestimate the observed rate of earthquake production at the beginning of the sequence. As far as the analysis of the second-class synthetic catalogs is concerned, the analysis of the residuals as performed in the real sequence (see previous sections) does not show any significant change point and rejection of the Poisson hypothesis as well. This is clearly shown in Figure 6, where we display the results of residuals analysis for a typical synthetic catalog together with values of parameters estimated by applying the method proposed by *Zhuang et al.* [2002].

The analysis of synthetic catalogs allows us to exclude that a bias in the background seismicity estimation is the main cause of the recognized increase of background rate in the early phase of the sequence. We conclude that these tests corroborate the hypothesis of a real variation of the background seismicity rate caused by physical processes affecting the loading rate. We exclude the contribution of postseismic viscoelastic relaxation of the lower crust, because it contributes to stress perturbations over longer temporal scales than the duration of the aftershock sequence. Indeed, the inferred change of background seismicity rate occurs within a month after the first main shock. Therefore, the most likely physical processes that can affect the background seismicity rate during the aftershock sequence are afterslip or poro-elastic relaxation. They have been both proposed in the literature to explain the seismicity pattern or the observed postseismic deformation (*Miller et al.*, 2004; *Antonioli et al.*, 2005; *Riva et al.*, 2007). *Miller et al.*, (2004) interpreted the evident SE migration of seismicity and the occurrence of normal faulting aftershocks on the hanging wall of the main shock fault planes in terms of pore pressure relaxation and proposed a model based on non-linear diffusion. Moreover, *Riva et al.* (2007) modeled GPS measurements of postseismic deformation in terms of viscoelastic relaxation and afterslip at the base of the seismogenic upper crust. They collected evidence of long-lasting afterslip following the Colfiorito main shocks. However, their postseismic measurements concern a time-window comprised between 3 and 5.5 years after the beginning of the 1997 earthquake sequence and their observed GPS

displacements are caused by a strain signal of the order of a few millimeters per year. Therefore, it is likely to exclude that such a long lasting afterslip can be the process leading to the inferred increase of background seismicity rate immediately following the first main shock.

We also exclude the contribution of shallow afterslip (that is, stable aseismic slip) in the upper kilometers of the main shocks fault plane [Marone *et al.*, 1991] for several reasons. First, the surface deformation is not the direct result of primary rupture of deep faults [Cinti *et al.*, 1999]. Second, afterslip immediately after the first main shocks was not observed despite the proximity of two GPS receivers to the September 26<sup>th</sup> main shock fault plane [see Hunstad *et al.*, 1999, among many others]. Third, several studies show that the temporal pattern of seismicity triggered by shallow afterslip is consistent with an Omori-type decay on a temporal scale ranging from days to months after the main shock [Wennerberg and Sharp, 1997; Hsu *et al.*, 2006; Helmstetter and Shaw, 2009]. The transient variation of background seismicity rate inferred in this study (Figure 5) does not match the Omori-like decay. Therefore, we conclude that the ETAS model would not include afterslip-triggered seismicity, if any, in the background rate (see equation 2).

According to these considerations, we believe that poro-elastic relaxation and fluid flow can represent the most likely physical mechanism perturbing the tectonic and coseismic stress fields. Indeed, pore pressure relaxation can have a temporal evolution comparable to the duration of the aftershock sequence. Moreover, this is a reasonable physical interpretation since deep fluids are present in the study area (Chiodini *et al.*, 2000), temporal variations of anisotropy have been observed during the sequence (Piccinini *et al.*, 2006) and because aftershocks have been modeled in terms of fluid driven triggering caused by coseismic elastic stress changes [Miller *et al.*, 2004; Antonioli *et al.*, 2005]. Physics-based models solely relying on elastic stress changes fail in reproducing both the spatial distribution of aftershocks and, more important, the spatio-temporal migration of seismicity (Cocco *et al.*, 2000; Nostro *et al.*, 2005; Catalli *et al.*, 2008). They are only able to explain the stress-interactions among the repeated sequence of main shocks, which in turn represent a likely driving mechanism for fluid flow.

In order to corroborate this interpretation we have compared the spatio-temporal distribution of background events selected through the ETAS model with the fluid diffusion model proposed by Shapiro *et al.* (2003) and applied by Antonioli *et al.* (2005) to the Umbria-Marche 1997 seismic sequence. According to this theoretical approach the spatial and temporal evolution of seismicity during the Umbria-Marche seismic sequence is modeled in terms of subsequent failures promoted by fluid flow. The diffusion process of pore-pressure relaxation is represented as a pressure perturbation generated by coseismic stress changes and propagating through a fluid saturated

medium. These authors proposed a solution of the Darcy's law for a step-function point-source pore pressure in a isotropic homogeneous fluid saturated medium and introduced the alternative notion of triggering front to model the spatio-temporal pattern of hydraulically induced seismicity. Following *Shapiro et al.* (1999, 2003), we adopt the following equation to define the triggering front:

$$r = \sqrt{D_{iso}\pi t} \quad (7)$$

where  $t$  is the time measured since the initiation of fluid intrusion,  $r$  is the distance from the point source and  $D_{iso}$  is the isotropic hydraulic diffusivity. This approach predicts that fluid flow may trigger an event at a location  $r$  at any time after the perturbation. Therefore, in a  $(r,t)$  plot, the earthquakes are expected to lie below the triggering front defined by equation (7).

To retrieve the spatial pattern of non self-triggered seismicity we declustered the catalog by using the stochastic procedure proposed by *Zhuang et al.* [2002]. The great majority of all events (87%) likely belong to self-triggered activity (i.e.  $\rho_i$  is larger than 0.9; see eq (5)); 11% of events have a probability  $\rho_i$  ranging from 0.1 to 0.9. Unlike conventional declustering methods, the random procedure proposed by *Zhuang et al.* [2002] does not make a fixed judgment on whether or not an event is an offspring. Therefore, by repeating random declustering, different stochastic copies of background seismicity can be produced. Some statistics can be calculated to evaluate a particular feature of the declustered seismicity. Here, we generate 1000 stochastic versions of a declustered catalog and for each of them we evaluate the agreement between the spatio-temporal distribution of events and the theoretical evolution of fluid induced seismicity predicted by relation (7). In particular, for each catalog we compute the maximum distance  $r_{max}$  from the first earthquake in a moving time window of 12 hours. Then, we check a linear relation between time and squared maximum distance ( $r_{max}^2$ ) by a regression analysis. The adoption of  $r_{max}$  is required by the condition that earthquakes can lie at any time below the triggering front defined by equation (7). The significance of this viable relation is tested by using the F-test, which allows us to verify the null hypothesis of uncorrelation between occurrence times and locations of events [*Draper and Smith, 1981*]. We have summarized in Table 3 the information concerning our regression analysis. In particular, we report the minimum and maximum values of goodness-of-fit parameter  $R^2$  for 1000 declustered catalogs. The distribution of  $R^2$  values is represented by mean and standard deviation. The same information is reported also for the isotropic diffusivity coefficient  $D_{iso}$  and for  $p$ -value of F-test. Ultimately we report the percentage of catalogs for which we reject the null hypothesis of uncorrelation between occurrence times and locations of events at 95% confidence level.

We find that the hypothesis of fluid driven seismicity is not statistically significant for the whole time period of the CAS (Sept. 3<sup>rd</sup> 1997 – Aug. 17<sup>th</sup> 1998). All parameters have very scattered

values for different declustered catalogs and only for 44% of cases we can reject the null hypothesis. The agreement between spatio-temporal evolution of seismicity and fluid diffusion model becomes clearer if we limit the investigation time window to the period characterized by the highest rate of earthquake production, which coincides with the occurrence of the main shocks that are believed to have triggered the fluid flow and the pore pressure relaxation process (*Antonioli et al.*, 2005; *Catalli et al.*, 2008). Indeed, we reject the null hypothesis for 100% of catalogs, if we only include in regression analysis those earthquakes occurred between September 26<sup>th</sup> and October 31<sup>st</sup> 1997 (this time period coincides with the most pronounced background seismicity variation, see Figure 5). In this last case the mean value of isotropic diffusivity  $D_{iso}$  is  $61 \pm 9 \text{ m}^2/\text{s}$ . This value is consistent with those inferred by *Antonioli et al.* (2005) for the aftershock catalog. We display in Figure 7 the spatio-temporal distribution for a random declustered catalog together with the pore-pressure triggering front envelope predicted by our regression, assuming the origin of the triggering front at the epicenter and origin time of the first September 26 main shock. This figure suggests that most of the background events lie below the triggering front with some exceptions at the beginning of the sequence. The latter feature can be due to two possible causes: 1) the difficulty of unequivocally identifying the beginning of the fluid flow or pore pressure relaxation and 2) a temporal variation of hydraulic diffusivity, following the occurrence of those causative main shocks that are able to modify fluid pressurization (*Antonioli et al.*, 2005).

## Discussion and conclusive remarks

In the present work we have analyzed by means of suitable statistical tools the spatio-temporal evolution of the 1997-98 Colfiorito sequence. The complexity of this aftershocks sequence, characterized by a repeated sequence of  $5.0 < M_L < 6.0$  main shocks each of which having its own aftershock sequence (*ChiaraLuce et al.*, 2003; 2004), has been investigated by recent studies mainly based on theoretical and numerical investigations. Several studies have shown that the elastic static Coulomb stress models are able to describe the main shocks triggering (*Cocco et al.*, 2000; *Nostro et al.*, 2005), but fail to explain the spatial pattern and the focal mechanisms of aftershocks (*Nostro et al.*, 2005; *Catalli et al.*, 2008). Specifically, these models are unable to explain the evident migration of seismicity towards SE, along the strike of the normal fault system, at nearly 1 km/day (*ChiaraLuce et al.*, 2003; *Miller et al.*, 2004). This particular feature has been mainly explained by the presence of deep fluid circulation and natural degassing (*Chiodini et al.*, 2000; *Antonioli et al.*, 2005), which are believed to have also caused the occurrence of aftershocks in the hanging-wall of the main normal fault planes (*Miller et al.*, 2004).

All these results have motivated us to investigate if statistical models are able to capture and to describe the complex spatio-temporal evolution of the 1997-98 Umbria-Marche sequence. To achieve this goal we have applied the ETAS model to the CSI1.1 catalog and, by adopting a rigorous statistical verification, we have shown that the ETAS model with a stationary background rate is unable to match the observed rate of earthquake production in a time window comprising the 1997-98 Colfiorito seismic sequence. We have therefore limited the application of the ETAS approach to those earthquakes belonging to this sequence (September 3<sup>rd</sup> 1997 - August 17<sup>th</sup> 1998). This second modeling attempt corroborated the inadequacy of the ETAS model with a stationary background rate to fit the observations. It emerges that the most likely explanation of this failure is the underestimation of the background seismicity rate. A more accurate inspection reveals that the background rate changes with time, showing a clear increase at the beginning of aftershock sequence (Figure 5). The inferred increase of background seismicity rate lasts for few months, in the period characterized by the occurrence of the largest magnitude shocks in the Colfiorito area, and its pronounced increase is simultaneous to the occurrence of the largest magnitude events. This further corroborates the finding that the main shocks activated the transient driving process causing the observed variations in background rate. We have also verified the presence of possible bias in the estimate of the background seismicity rate changes by analyzing synthetic seismic catalogs appositively generated to this task. The result of this synthetic test corroborates that our estimates of background rate are not biased and that the inferred increase is a real feature of the observed rate of earthquake production.

Our interpretation of these results relies on the transient effects caused by fluid flow and pore pressure relaxation, which represent the perturbation to the stress state of the crust and are promoted by the coseismic stress changes generated by repeated main shocks. Pore pressure relaxation is believed to be the most reliable explanation for the observed variation of the background rate. In order to support this interpretation we have compared the background seismicity selected through the ETAS model with the fluid flow poroelastic model proposed by *Shapiro et al.* (2003) and applied by *Antonioli et al.* (2005) to the Colfiorito aftershock sequence. Both the visual comparison and a statistical test confirm that the spatio-temporal evolution of background seismicity is consistent with this poro-elastic model. In particular, the statistical analysis demonstrates that this agreement is quite robust if we limit our analysis to the time period characterized by the occurrence of the main shocks that are considered the driving causative mechanism (*Miller et al.*, 2004). Furthermore, the inferred range of likely values of isotropic diffusivity parameter is consistent with the estimates obtained by *Antonioli et al.* (2005) analyzing an independent data set ( $37 \leq D_{iso} \leq 92 \text{ m}^2/\text{s}$ ).

According to these results the earthquakes belonging to the background seismicity should display the same spatial migration observed for the coseismically-triggered aftershocks. We have verified that this is the case and we have plotted the results in Figure 8. This figure shows that: (i) background seismicity rate in the focal region (which comprises the area between Colfiorito and Sellano) was nearly constant before September 3<sup>rd</sup>, when the foreshock activity began, and afterwards the background rate increased near Colfiorito; (ii) from September 26<sup>th</sup> to October 9<sup>th</sup> the background rate near Colfiorito continuously increased and seismicity began to migrate to the SE toward Sellano; (iii) from October 10<sup>th</sup> to 20<sup>th</sup> 1997 the background seismicity rate is enhanced between Colfiorito and Sellano and in this period we observed the highest background rate (see Figure 5), which is therefore associated with the whole seismogenic volume activated during the sequence. After October 20<sup>th</sup> the background seismicity rate remained higher than the reference value before the beginning of the sequence, but it was decreasing back to its stationary level (see Figure 5). We have plotted the position of the triggering front in Figure 8, estimated by eq. (7) and considering the mean value of  $D_{iso}$  ( $61 \text{ m/s}^2$ ; see Table 3), superimposed to the spatial pattern of background rate in the different time windows. This comparison reveals that the time evolution of background rate is consistent with the propagation of a pore pressure perturbation in a fluid saturated medium. We are aware that hydraulic diffusivity is likely to be anisotropic (see Antonioli et al., 2005). However, we do not investigate this issue more in detail because it is beyond the goals of this work. We emphasize that in Figure 8 we plot the background seismicity rate density and that the spatial pattern of enhanced background rate is measured and plotted without assuming any anisotropic distribution. We believe that this is a further convincing observational evidence of the southeastward migration of seismicity during the Colfiorito sequence.

These results have relevant implications for the modeling of the rate of earthquake production through physics-based (Dieterich, 1994; Gomberg et al., 2005) and statistical approaches (Ogata, 1998). Indeed, most of applications of the rate and state dependent friction model (Toda et al., 1998; Toda and Stein, 2003, among many others) assume a constant background seismicity rate as a steady reference state preceding the coseismic stress perturbations. Our study presents new evidence suggesting the need to take into account a non-stationary background seismicity rate (see Hainzl and Ogata, 2005, Lombardi et al., 2006, Llenos et al., 2009). Moreover, the present study demonstrates that imaging the perturbative stress history through multiple stress steps solely associated with the largest magnitude earthquakes might not always be appropriated (see also Nostro et al., 2005; Catalli et al., 2008). It provides further observational evidence that fluids (fluid flow and/or pore pressure relaxation) can contribute to the complex stress time history

triggering earthquakes during tectonic seismic sequences. Recently, *Llenos et al.* (2009) pointed out the role of aseismic transient processes (such as afterslip or aseismic slip) on background seismicity rate in earthquake swarms. In agreement with *Lombardi et al.* (2006) and *Llenos et al.* (2009), we argue that the ETAS model enables us to separate the coseismically and the aseismically-triggered seismicity over a short-time period.

Our findings open new perspectives for a reliable estimation of background seismicity rate, required to perform retrospective or prospective forecasting attempts of the rate of earthquake production (see for instance *Woessner et al.*, 2009; *Hainzl et al.*, 2009). To this task, *Hainzl et al.* [2009] have recently proposed to estimate the background rate by including the early aftershocks of a sequence. Here we show that a non-stationary background rate can characterize the aftershock sequence and further complicate such an estimate. Finally, in addition to the results found by *Hainzl and Ogata* (2005) and *Lombardi et al.*, (2006) investigating seismic swarms, the present study shows that taking into account the spatio-temporal variation of background rate can provide a robust evidence of fluid-driven triggered seismicity.

## Data and Resources

The earthquake catalog data were obtained from <http://csi.rm.ingv.it>. The maps were made using the Generic Mapping Tools ([www.soest.hawaii.edu/gmt](http://www.soest.hawaii.edu/gmt))

## Acknowledgments

The researches that motivated this study have been promoted in the framework of two EC projects, namely NERIES (Network of Research Infrastructures for European Seismology, [www.neries-eu.org](http://www.neries-eu.org)) and SAFER (Seismic Early Warning for Europe, [www.saferproject.net](http://www.saferproject.net)). This work is part of the EU-project SAFER, contract 036935. We thank Sebastian Hainzl, Jochen Woessner and Stefan Wiemer for useful discussions. A.M. Lombardi has been supported by the EC project NERIES contract 026130.

## References

- Antonioli A., M. E. Belardinelli and M. Cocco (2004), Modeling Dynamic Stress Changes Caused by an Extended Rupture in an Elastic Stratified Half Space, *Geophys. J. Int.*, 157, 1, 229-244.

Antonioli A., Piccinini D., Chiaraluce L. and M. Cocco (2005), Fluid flow and seismicity pattern: evidence from the 1997 Umbria-Marche (central Italy) seismic sequence, *Geophys. Res. Lett.*, 32, L10311, doi:10.1029/2004GL022256.

Catalli, M. Cocco, R. Console, and L. Chiaraluce (2008). Modeling seismicity rate changes during the 1997 Umbria-Marche sequence (central Italy) through a rate- and state-dependent model, *J. Geophys. Res.*, 113, doi:10.1029/2007JB005356.

Castello B., G. Selvaggi, C. Chiarabba and A. Amato (2005), CSI Catalogo della sismicità italiana 1981-2002, vers. 1.0, INGV-CNT, Roma, [www.ingv.it/CSI/](http://www.ingv.it/CSI/).

Castello B., M. Olivieri and G. Selvaggi (2007), Local and Duration Magnitude Determination for the Italian Earthquake Catalog, 1981-2002, *Bull. Seism. Soc. Am.*, 97, 128-139.

Chiaraluce L., Ellsworth W.L., Chiarabba C. and M. Cocco (2003), Imaging the complexity of an active normal fault system: the 1997 Colfiorito (central Italy) case study, *J. Geophys. Res.*, 108, (B6) 2294, doi:10.1029/2002JB002166.

Chiaraluce L., A. Amato, M. Cocco, C. Chiarabba, G. Selvaggi, M. Di Bona, D. Piccinini, A. Deschamps, L. Margheriti, F. Courboulex, and M. Ripepe (2004), Complex Normal Faulting in the Apennines Thrust-and-Fold Belt: The 1997 Seismic Sequence in Central Italy, *Bull. Seism. Soc. Am.*, 94(1), 99-116.

Chiodini G., Frondini F., Cardellini C. and L. Peruzzi (2000), Rate of diffuse carbon dioxide earth degassing estimated from carbon balance of regional aquifers: the case of central Apennine, Italy, *J. Geophys. Res.*, 105, 8423-8434.

Cinti F.R., Cucci L., Marra F. and P. Montone (1999). The 1997 Umbria Marche (Italy) earthquake sequence: relationship between ground deformation **and seismogenic structure**, *Geophys. Res. Lett.*, 26, NO.7, 895-898.

Cocco, M., C. Nostro, and G. Ekstrom (2000), Static stress changes and fault interaction during the 1997 Umbria-Marche earthquake sequence, *J. Seismol.*, 4 (4), 501-516.

Console R., M. Murru and A.M. Lombardi (2003), Refining earthquake clustering models, *J. Geophys. Res.*, 108(B10), 2468, doi:10.1029/2002JB002130.

Daley D.J. and D. Vere-Jones (2003), *An Introduction to the Theory of Point Processes*, Springer-Verlag, New York, 2-nd ed., Vol. 1, pp. 469.

Dieterich, J.H. (1992), Earthquake nucleation on faults with rate-and-state dependent strength, *Tectonophysics*, 211, 115-134,.

Dieterich, J.H. (1994), A constitutive law for rate of earthquake production and its application to earthquake clustering, *J. Geophys. Res.*, 99, (18):2601-2618.

Draper N.R. and H Smith (1981), *Applied regression analysis*, J. Wiley, New York, 2-nd ed., pp. 709,.

Felzer, K. R., R. E. Abercrombie, and G. Ekström (2003), Secondary aftershocks and their importance for aftershock prediction, *Bull. Seis. Soc. Am.*, 93, 1433-1448.

Freed A.M. (2005), Earthquake triggering by static, dynamic, and post-seismic stress transfer. *Ann Rev Earth Planet Sci* 33, 335-367.

Gerstenberger, M.C., Wiemer, S., Jones, L.M., and Reasenberg (2005), P. A., Real-time forecasts of tomorrow's earthquakes in California, *Nature*, 435, 328-331.

Gibbons, J.D. and S. Chakraborti (2003), Non-parametric Statistical Inference, 4th ed., rev. and expanded, New York: Marcel Dekker, 645 pp.

Gomberg J. and P. Jonhson (2005), Dynamic triggering of earthquakes, *Nature*, 437, 830, doi:10.1038/nature04167.

Gomberg, J., P. Reasenberg, N. Beeler, M. Cocco, and M. E. Belardinelli (2005), A frictional population model of seismicity rate change, *J. Geophys. Res.*, 110 (B05S03), doi:10.1029/2004JB003404.

Hainzl S. and Y. Ogata (2005), Detecting fluid signals in seismicity data through statistical earthquake modeling, *J. Geoph. Res.* 110, B05S07, doi:10.1029/2004JB003247.

Hainzl, S., Enescu, E., Cocco, M., Woessner, J., Catalli, C., Wang, R., and Roth, F. (2009), Forecasting aftershock seismicity Part II: Aftershock modeling based on uncertain stress calculations, in press on *J. Geophys. Res.*

Harris, R. (1998), Introduction to special section: stress triggers, stress shadows, and implications for seismic hazard, *J. Geoph. Res.* 103 (B10), 24,347–24, 358,

Helmstetter A. and D. Sornette (2002), Sub-critical and supercritical regimes in epidemic models of earthquake aftershocks, *J. Geophys. Res.* 107, B10, 2237, doi:10.1029/2001JB001580.

Helmstetter and D. Sornette (2003), Importance of direct and indirect triggered seismicity in the ETAS model of seismicity, *Geophys. Res. Lett.* 30 (11), doi:10.1029/2003GL017670.

Helmstetter A., Y. Y. Kagan and D. D. Jackson (2005), Importance of small earthquakes for stress transfer and earthquake triggering, *J. Geoph. Res.* 110, B05S08, doi:10.1029/2004JB003286.

Helmstetter A. and B.E. Shaw (2009), Afterslip and aftershocks in the rate-and-state friction law, *J. Geophys. Res.*, 114, B01308, doi:10.1029/2007JB00577.

Hill D.P., Reseanberg P.A., Michael A., Arabaz W.J., Beroza G., Brumbaugh D., Brune J.N., Castro R., Davis S., dePolo D., Ellsworth W.L., Gomberg J., Harmsen S., House L., Jackson S.M., Johnston M.J.S., Jones L., Keller R., Malone S., Munguia L., Nava S., Pechmann J.C., Sanford A., Simpson R.W., Smith R.B., Stark M., Stickney M., Vidal A., Walter S., Wong V., Zollweg J. (1993), Seismicity Remotely Triggered by the Magnitude 7.3 Landers, California, Earthquake, *Science*, 260, 1617-1623, 1993.

Hsu Y.J., Simons M., Avouac J.P., Galetzka J., Sieh K., Chlieh M., Natawidjaja D., Prawirodirdjo L. and Y. Bock (2006), Frictional Afterslip Following the 2005 Nias-Simeulue Earthquake Sumatra, *Science*, 312, 1921-1926, doi:10.1126/science.1126960.

Hunstad I., Anzidei M., Cocco M., Baldi P., Galvani A. and A. Pesci (1999). Modeling coseismic displacements during the 1997 Umbria-Marche earthquake (central Italy), *Geophys. J. Int.*, 139, 283-295.

Hurvich, C. M., and C.-L. Tsai (1989), Regression and time series model selection in small samples, *Biometrika*, 76, 297 – 307.

Kagan Y.Y. and D.D. Jackson (2000), Probabilistic forecasting of earthquakes, *Geophys. J. Int.*, 143, 438-453.

Kilb, D., J. Gomberg and P. Bodin (2000), “Triggering of earthquake aftershocks by dynamic stresses,” *Nature*, 408, 570-574.

King, G.C.P., Stein R.S. and J. Lin (1994), Static stress changes and the triggering of earthquakes, *Bull. Seism. Soc. Am.*, 84, 935-953.

King, G.C.P., and M. Cocco (2000), Fault interaction by elastic stress changes: New clues from earthquake sequences, *Adv. Geophys.* 44, 1-38.

Kisslinger C. and L.M. Jones (1991), Properties of aftershocks in southern California, *J.Geophys. Res.* 96, 11947-11958.

Llenos ,A.L., McGuire J.J. and Y. Ogata (2009), Modeling seismic swarms triggered by aseismic transient, *Earth Planet. Sc. Lett.*, 281, 59-69.

Lombardi A.M., Marzocchi W. and J. Selva (2006), Exploring the evolution of a volcanic seismic swarm: The case of the 2000 Izu Islands swarm, *Geophys. Res. Lett.*, 33, L07310, doi:10.1029/2005GL025157.

Lombardi, A. M., and W. Marzocchi (2007), Evidence of clustering and nonstationarity in the time distribution of large worldwide earthquakes, *J. Geophys. Res.*, 112, B02303, doi:10.1029/2006JB004568.

Manga, M., and C.-Y. Wang, *Earthquake hydrology*, in *Treatise on Geophysics*, G. Schubert editor,

4, 293-320, 2007

Marone, C.J., Scholz, C.H. and R. Bilham (1991). On the mechanics of earthquake afterslip *J. Geophys. Res.*, 96, B5, 8441-8452.

Marzocchi W. (2008), Earthquake forecasting in Italy, before and after Umbria-Marche seismic Sequence 1997. A review of the earthquake occurrence modeling at different spatio-temporal-magnitude scales. *Ann. Geophys.*, 51, 87-98.

Marzocchi W., A.M. Lombardi (2008), A double branching model for earthquake occurrence. *J. Geophys. Res.*, 113, B08317, doi:10.1029/2007JB005472.

Miller S.A., C. Collettini, L. Chiaraluce, M. Cocco, M. Barchi and B.J.P. Kaus (2004), Aftershocks driven by a high-pressure CO<sub>2</sub> source at depth, *Nature*, 427, 724-727.

Mogi K. (1967), Earthquakes and fractures, *Tectonophysics* 5, 35-55.

Mulargia F., and S. Tinti (1985), Seismic sample areas defined from incomplete catalogues: an application to the Italian territory, *Phys. Earth Planet. Int.* 40, 273-300.

Nostro, C., L. Chiaraluce, M. Cocco, D. Baumont, and O. Scotti (2005), Coulomb stress changes caused by repeated normal faulting earthquakes during the 1997 Umbria-Marche (central Italy) seismic sequence, *J. Geophys. Res.*, 110 (B05S20), doi:10.1029/2004JB003386.

Nur A. and J.R. Booker (1972), Aftershocks caused by pore fluid flow?, *Science*, 175, 885-887.

Ogata Y., Statistical Models for Earthquake Occurrences and Residual Analysis for Point Processes, *J. Amer. Statist. Assoc.* 83(401), 9-27, 1988.

Ogata Y. (1992), Detection of precursory relative quiescence before great earthquakes through a statistical model, *J. Geophys. Res.* 97, 19,845-19,871.

Ogata Y. (1998), Space-Time Point-Process Models for Earthquake Occurrences, *Ann. Inst. Statist. Math.* 50(2), 379-402,

Ogata, Y. (2005a), Detection of anomalous seismicity as a stress change sensor, *J. Geophys. Res.*, 110, B5, B05S06, doi:10.1029/2004JB003245.

Ogata, Y. (2005b), Synchronous seismicity changes in and around the northern Japan preceding the 2003 Tokachi-oki earthquake of M8.0, *J. Geophys. Res.*, 110, B5, B08305, doi:10.1029/2004JB003323.

Ogata, Y. (2006), Monitoring of anomaly in the aftershock sequence of the 2005 earthquake of M7.0 off coast of the western Fukuoka, Japan, by the ETAS model, *Geophys. Res. Lett.*, 33, 1, L01303, doi:10.1029/2005GL024405.

Ogata Y. and J. Zhuang (2006), Space-time ETAS models and an improved extension, *Tectonophys.* 413, 13-23.

Piccinini D. , Margheriti L. , Chiaraluce L. , Cocco M. (2006), Space and time variation of crustal anisotropy during the 1997 Umbria-Marche, central Italy, seismic sequence, *Geophys. J. Int.*, 167, 1482-1490, DOI: 10.1111/j.1365-246X.2006.03112.x.

Piersanti A., G. Spada, R. Sabadini, and M. Bonafede (1995), Global postseismic deformation, *Geophys. J. Int.*, 120, 544-566.

Pollitz F.F. (1992), Postseismic relaxation theory on the spherical Earth, *Bull. Seismol. Soc. Am.*, 82, 422-453.

Pollitz, F.F., R. Burgmann and P. Segall (1998), Joint estimation of afterslip rate and postseismic relaxation following the 1989 Loma Prieta earthquake, *J. Geophys. Res.*, 103, B11, 26,975-26,992.

Shapiro, S. A., P. Audigane, and J. J. Royer (1999), Large scale in situ permeability tensor of rocks from induced microseismicity, *Geophys. J. Int.*, 137, 207 – 213.

Shapiro, S. A., R. Patzig, E. Rothert, and J. Rindshwentner (2003), Triggering of seismicity by pore-pressure perturbations: Permeability-related signature of the phenomenon, *Pure Appl. Geophys.*, 160, 1051-1066.

Sornette D. and M.J.Werner (2005), Apparent clustering and apparent background earthquakes biased by undetected seismicity, *J.Geophys. Res.* 110, B09303, doi:10.1029/2005JB003621.

Steacy, S., J. Gomberg, and M. Cocco (2005), Introduction to special section: stress transfer, earthquake triggering, and time-dependent seismic hazard, *J. Geophys. Res.*, 110 (B05S01), doi:10.1029/2005JB003692.

Stein R.S. (1999), The role of stress transfer in earthquake occurrence, *Nature*, 402, 605-609.

Toda, S., Stein, R.S., Reaseanberg, P.A., Dieterich, J.H. and Yoshida, A. (1998), Stress transferred by the 1995 Mw=6.9 Kobe, Japan, shock: effect on aftershocks and future earthquake probabilities, *J. Geophys. Res.*, 103, 24543-24565.

Toda, S., and R. S. Stein (2003), Toggling of seismicity by the 1997 Kagoshima earthquake couplet: A demonstration of time-dependent stress transfer, *J. Geophys. Res.* 109 (B12, 2567), doi:10.1029/2003JB002527.

Toda, S., R. S. Stein, K. Richards-Dinger, and S. B. Bozkurt (2005), Forecasting the evolution of seismicity in southern California: animations built ion earthquakes stress transfer, *J.Geophys. Res.*, 110, B05S16, doi:10.1029/2004JB003415.

Utsu T. and A. Seki (1955), Relation between the area of aftershock region and the energy of the main shock (in Japanese), *Zisin (J. Seismol. Soc. Japan)*, 2nd Ser., ii 7, 233-240.

Utsu T., Ogata Y. and R.S. Matsu'ura (1995), The centenary of the Omori formula for a decay law of aftershocks activity, *J. Phys. Earth.*, 43, 1-33.

Wennerberg, L. and R.V. Sharp (1997), Bulk-friction modeling of afterslip and the modified Omori law, *Tectonophys.*, 277, 109-136, 1997.

Wiemer, S. (2001), A software package to analyze seismicity: ZMAP, *Seism. Res. Lett.*, 72, 373-382.

Wiemer, S., and M. Wyss (2000), Minimum magnitude of complete reporting in earthquake catalogs: examples from Alaska, the Western United States and Japan, *Bull. Seism. Soc. Am.*, 90, 859-869.

Wiemer, S., and M. Wyss (2002), Mapping spatial variability of the frequency-magnitude distribution of earthquakes, *Advances in Geophysics*, 45, 259-302.

Wössner, J., Wiemer, S. (2005), Assessing the quality of earthquake catalogues: Estimating the magnitude of completeness and its uncertainty. *Bull. Seism. Soc. Am.* 95, 684-698.

Woessner J., S. Hainzl, W. Marzocchi, M. J. Werner, A. M. Lombardi, F. Catalli, B. Enescu, M. Cocco, M. C. Gerstenberger and S. Wiemer (2009), Forecasting aftershock seismicity part III: A retrospective comparative test for the 1992 Landers sequence, submitted to *J. Geophys. Res.*

Zhuang J., Y. Ogata and D. Vere-Jones (2002), Stochastic declustering of space-time earthquake occurrence, *J. Am. Stat. Assoc.*, 97, 369-380.

Zhuang J., Ogata Y. and Vere-Jones D. (2004), Analyzing earthquake clustering features by using stochastic reconstruction, *J. Geophys. Res.*, 109, No. B5, B05301, doi:10.1029/2003JB002879.

Zhuang J., Chang C.P., Ogata Y. and Y.I. Chen (2005), A study on the background and clustering seismicity in the Taiwan region by using point process models, *J. Geophys. Res.* 110, B05S18, doi:10.1029/2004JB003157.

Zuniga F.R. and S. Wiemer (1999), Seismicity Patterns: Are they Always Related to Natural Causes?, *Pure appl. geophys.*, 155, 713-726.

## Table Captions

**Table 1:** Maximum Likelihood parameters (with relative errors) and log-likelihood of ETAS model for whole Umbria-Marche seismicity ( $M_c = 2.5$ ; Jan 1 1981 – Dec 31 2002; 1586 events).

**Table 2:** Maximum Likelihood parameters (with relative errors) and log-likelihood of ETAS model for 1997-1998 Umbria-Marche sequence ( $M_c = 2.5$ ; May 3 1997 – Aug 17 1998; 874 events).

**Table 3:** Regression Analysis on 1000 random stochastic versions of declustered catalog including the Umbria-Marche sequence, to test the reliability of the fluid diffusion model proposed by [Shapiro *et al.*, 1999; 2003]. The regression analysis is performed for the whole sequence (Sep 3 1997- Aug 17 1998) and for the first month of the sequence after the first main shock (Sept 26<sup>th</sup> 1997-Oct 31<sup>th</sup> 1997) in which a significant increase of background rate has been detected (see text for details).

## Figure Captions

**Figure 1:** Map of seismic events occurred in the Umbria-Marche region [ $12^{\circ}$ - $13.5^{\circ}$ W,  $42^{\circ}$ - $44^{\circ}$ N], from Jan 1 1981 to Dec 31 2002, with  $M_L \geq 1.5$  (12163 events). Solid circles indicate the events with  $M_L \geq 5.0$ . The first shock, occurred on April 29<sup>th</sup> 1984 (yellow square), while all the others belong to 1997-1998 Umbria-Marche sequence; the focal mechanisms of these events are also shown.

**Figure 2:** Estimate of completeness magnitude for Umbria-Marche seismicity (from Jan 1<sup>st</sup> 1981 to Dec 31<sup>st</sup> 2002) by MAXC method [Woessner and Wiemer, 2005]. a) Frequency magnitude distribution for the Umbria-Marche seismicity. The application of MAXC method provides  $M_c=1.7$ . b)  $M_c$  as function of time.

**Figure 3:** Cumulative number of transformed times  $\tau_i$  (top) and cumulative background seismicity (bottom) obtained by ETAS modeling for Umbria-Marche seismicity assuming  $M_c=2.5$ , occurred from Jan 1<sup>st</sup> 1981 to Dec 31<sup>st</sup> 2002. Vertical dotted lines mark change points identified by using the procedure proposed by Mulargia and Tinti [1985].

**Figure 4:** Comparison between the observed and predicted number of events for Umbria-Marche sequence for earthquakes above  $M_c=2.5$  (top panel) and  $M_c=3.0$  (bottom panel).

**Figure 5:** Temporal evolution of background seismic rate ( $v(t)$ ) for Umbria-Marche sequence for events above  $M_c=2.5$  (top) and  $M_c=3.0$  (bottom). The background rate is estimated for time interval of 5 and 10 days (dashed and solid lines, respectively).

**Figure 6:** Residual analysis for events above  $M_c=2.5$  belonging to a synthetic dataset with same length of the original whole catalog (Jan 1<sup>st</sup> 1981- Dec 31<sup>st</sup> 2002) and with a minimum magnitude equal to 1.0. The parameters of the ETAS model estimated using a completeness magnitude equal to 2.5 are listed.

**Figure 7:** Spatio-temporal distribution of background events for 1997-1998 Umbria-Marche sequence. Distances from the first main shock (Sept 26<sup>th</sup> 1997,  $M_I=5.6$ ) are plotted as a function of the occurrence times. Solid line refers to the theoretical position of the propagating pore pressure

front in the case of an isotropic hydraulic diffusivity of  $D_{iso}=59\ m^2/s$  estimated by regression analysis (see text for details).

**Figure 8:** Spatial distribution of background seismicity for different time windows in the Umbria-Marche region. The spatio-temporal evolution of background seismicity is estimated by using a nonstationary version of ETAS model (interval time of 5 days) and following the strategy adopted by *Lombardi et al.* (2006). The cumulative value of background rate ( $v(t)$ ) for the whole area is reported for each map. We have also drawn the position of the triggering front in different time windows estimated from equation (7) ( $D_{iso}=61\ m/s^2$ , see Table 3).

**Table1:** Parameters of ETAS model for whole Umbria-Marche seismicity  
 $(M_c = 2.5$ ; Jan 1 1981 – Dec 31 2002; 1586 events)

Parameter	Value
v	$0.055 \pm 0.003 (\text{day}^{-1})$
K	$0.033 \pm 0.003 (\text{day}^{p-1})$
p	$1.27 \pm 0.02$
c	$0.04 \pm 0.01 (\text{day})$
$\alpha$	$1.3 \pm 0.1 (\text{mag}^{-1})$
d	$0.7 \pm 0.1 (\text{km})$
q	$\equiv 1.5$
$\gamma$	$0.30 \pm 0.05 (\text{mag}^{-1})$
Log-likelihood	-12244.1

**Table2:** Parameters of ETAS model for 1997-1998 Umbria-Marche sequence  
 $(M_c = 2.5; \text{May 3 1997} - \text{Aug 27 1998}; 874 \text{ events})$

Parameter	Value
$\nu$	$0.13 \pm 0.02 (\text{day}^{-1})$
$K$	$0.05 \pm 0.01 (\text{day}^{p-1})$
$p$	$1.32 \pm 0.04$
$c$	$0.05 \pm 0.01 (\text{day})$
$\alpha$	$1.1 \pm 0.1 (\text{mag}^{-1})$
$d$	$0.5 \pm 0.1 (\text{km})$
$q$	$\equiv 1.5$
$\gamma$	$0.4 \pm 0.1 (\text{mag}^{-1})$
Log-likelihood	-3889.9

**Table 3.** Regression Analysis for 1000 stochastic version of declustered catalog.

	<b>Parameter</b>	<b>Min</b>	<b>Max</b>	<b>Mean</b>	<b>Std</b>	<b>% rejection (s.l. 5%)</b>
Sep 3 1997- Aug 17 1998	R <sup>2</sup>	8%	100%	80%	30%	44%
	D <sub>iso</sub> (m <sup>2</sup> /s)	1.2	69.1	32.6	22.2	
	p-value	0	0.68	0.11	0.18	
Sep 26 1997- Oct 31 1997	R <sup>2</sup>	28%	61%	44%	5%	100%
	D <sub>iso</sub> (m <sup>2</sup> /s)	36.6	92.2	61.2	8.9	
	p-value	0.0	0.0	0.0	0.0	

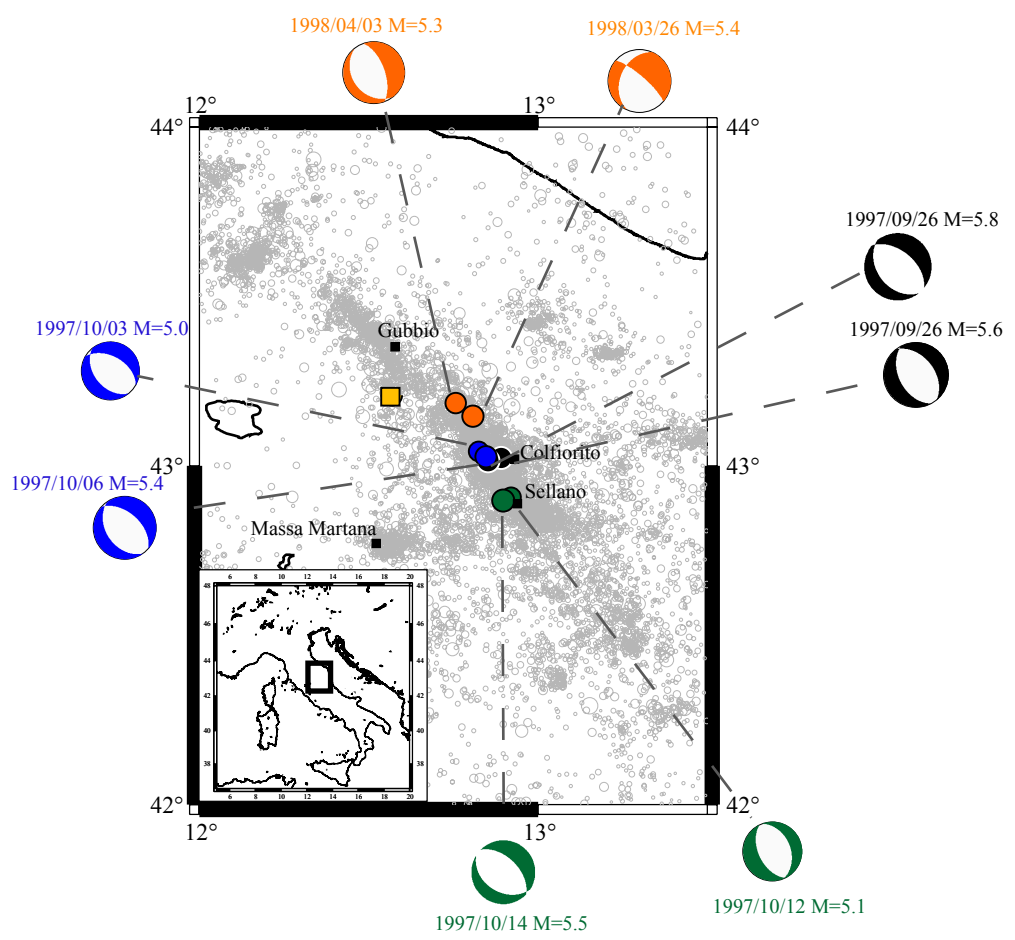


Figure 1

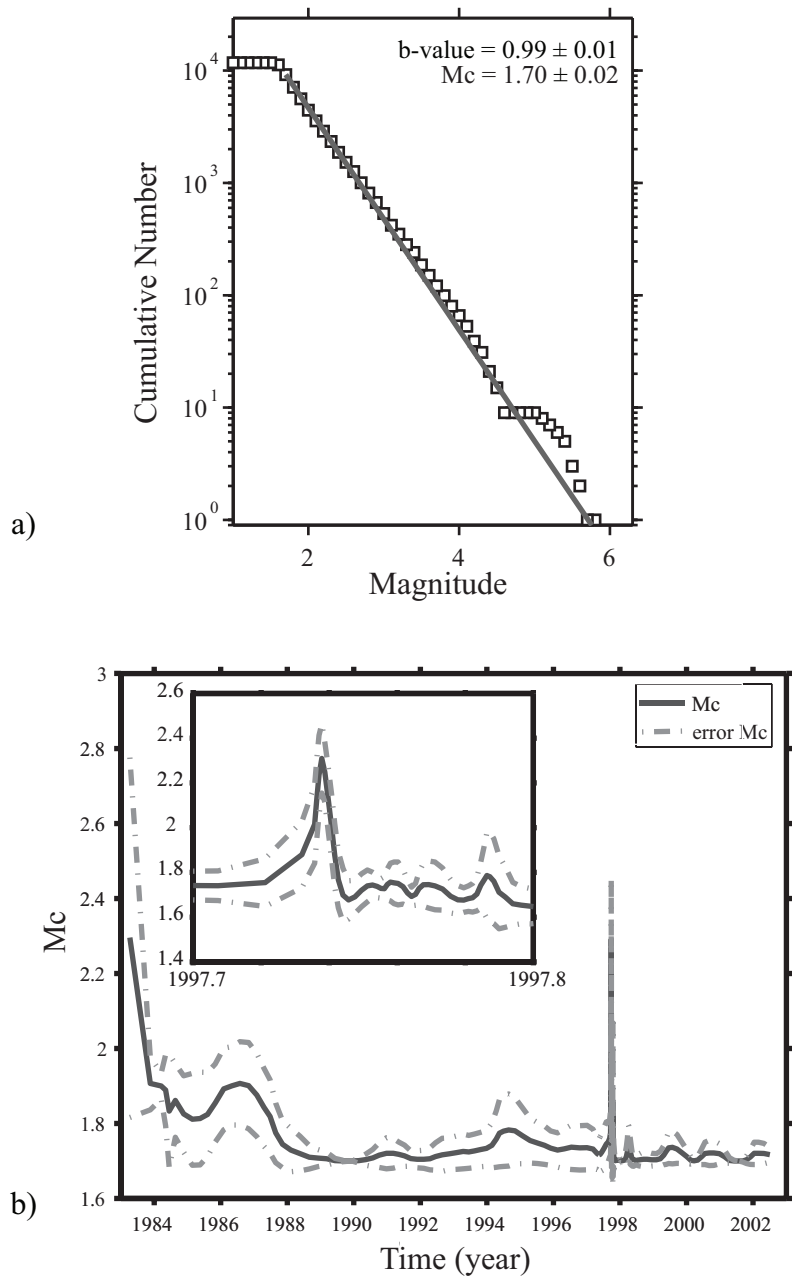


Figure 2

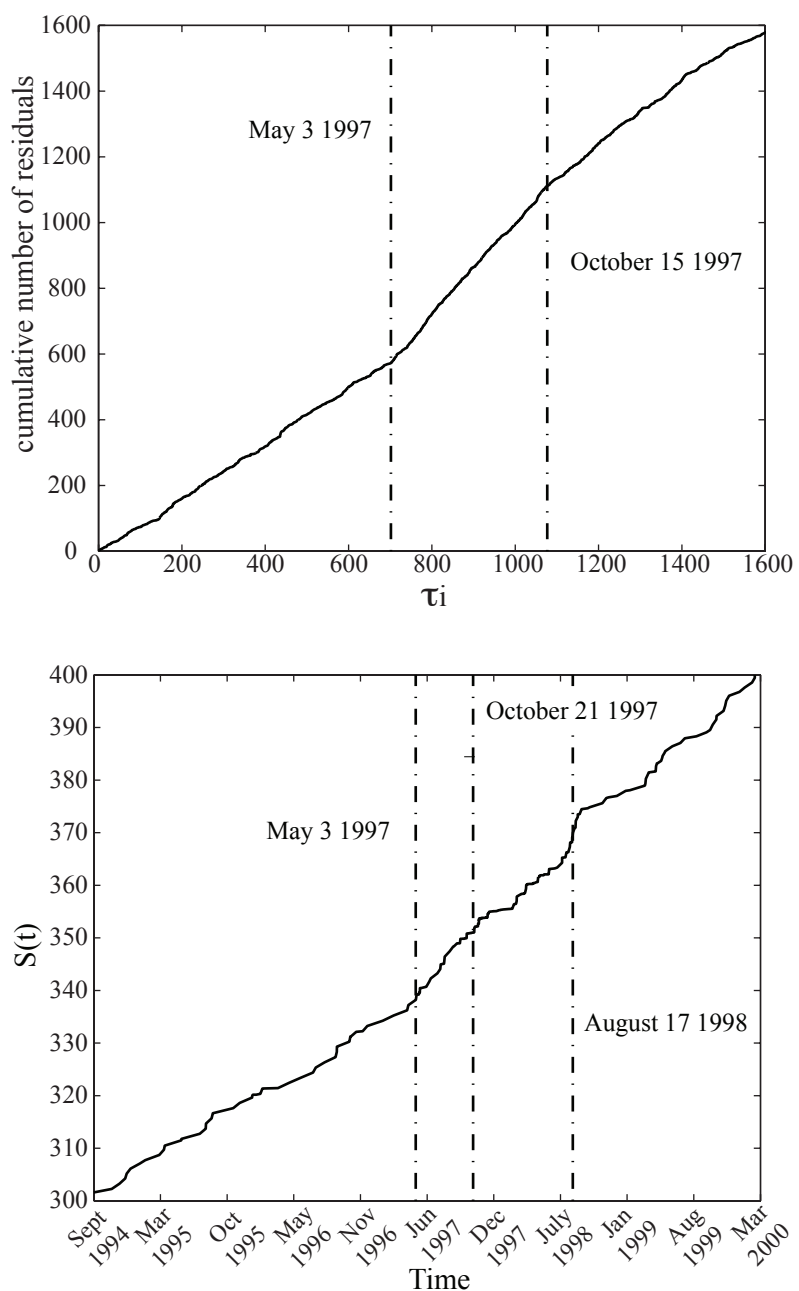


Figure 3

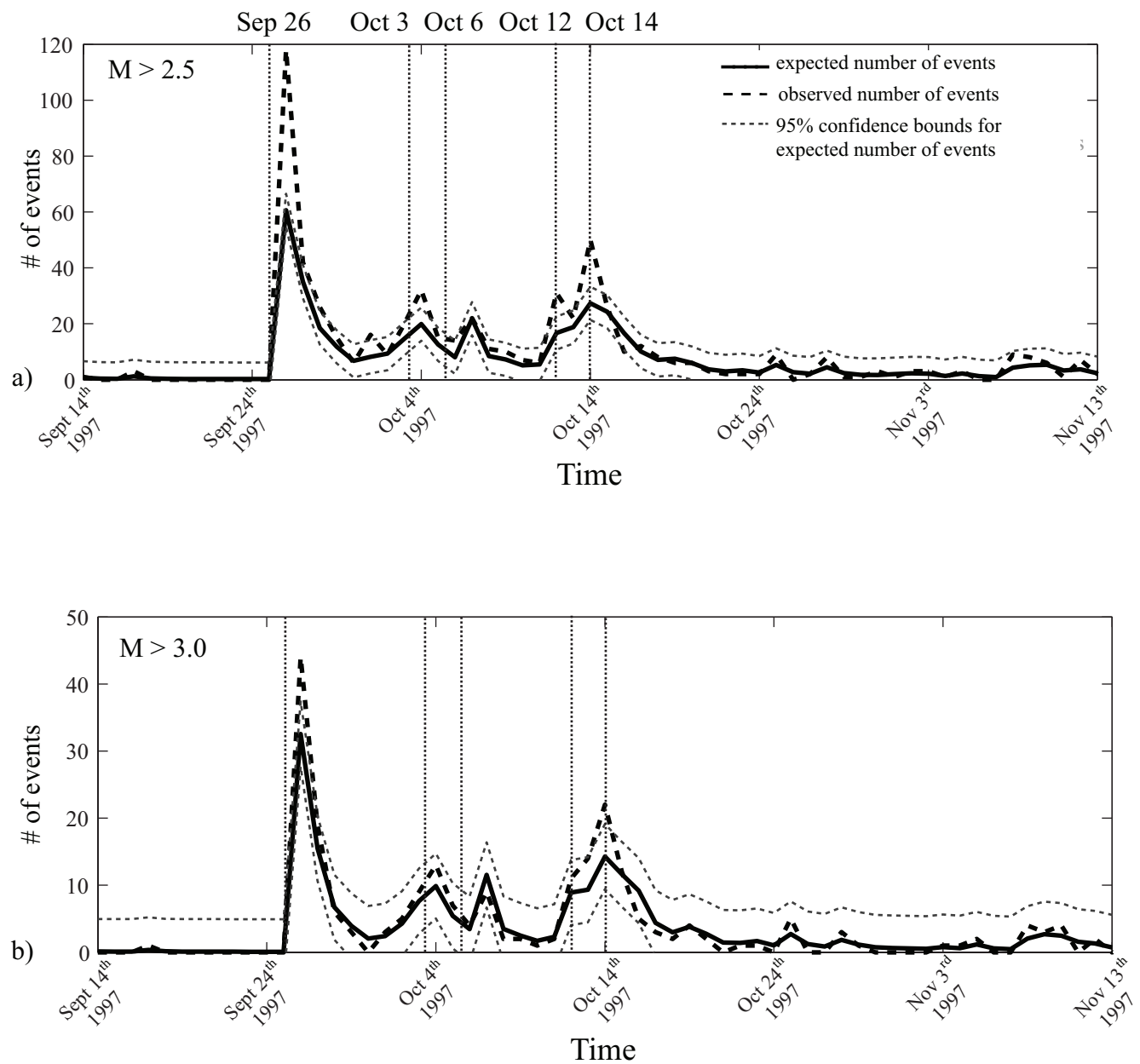


Figure 4

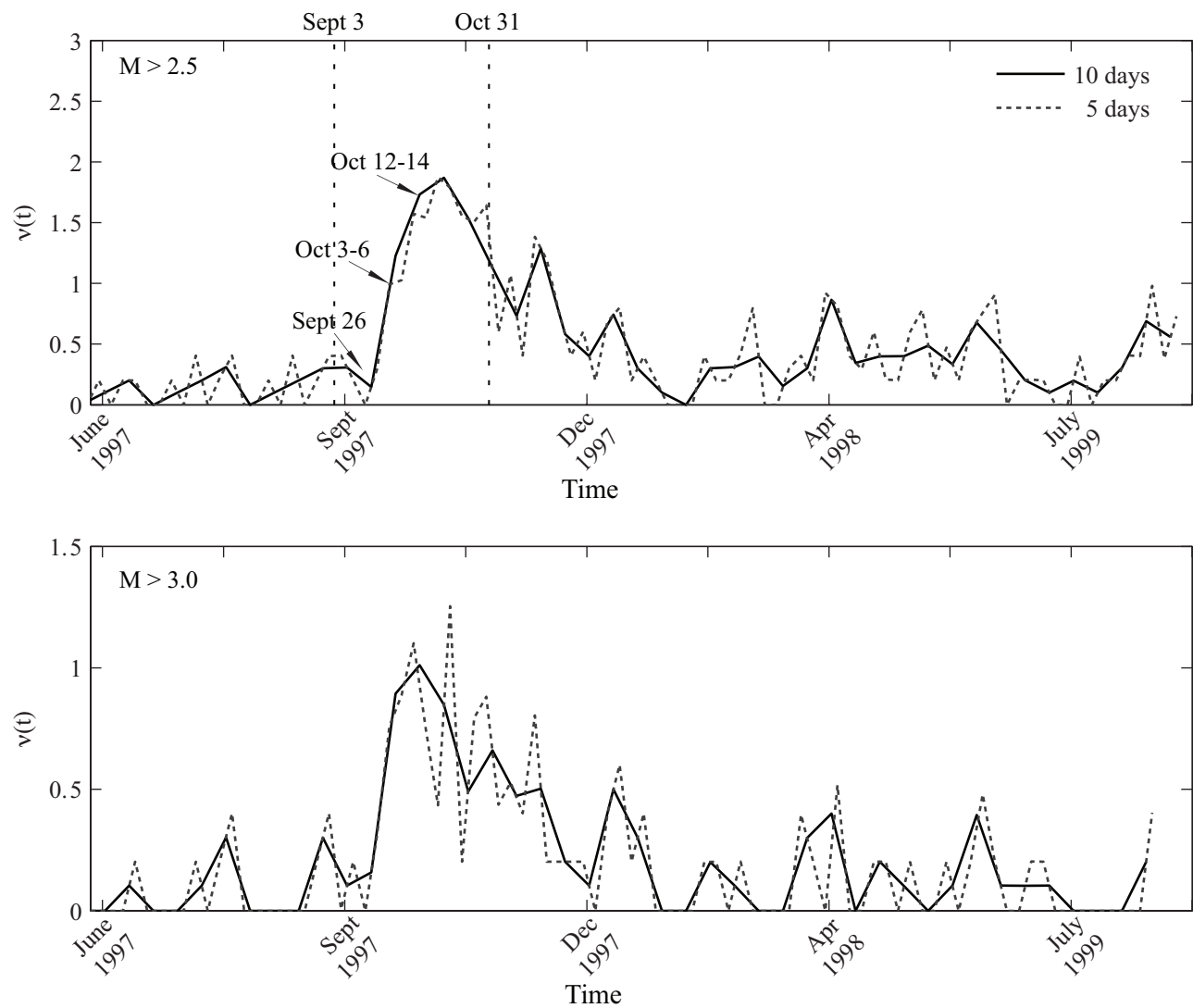


Figure 5

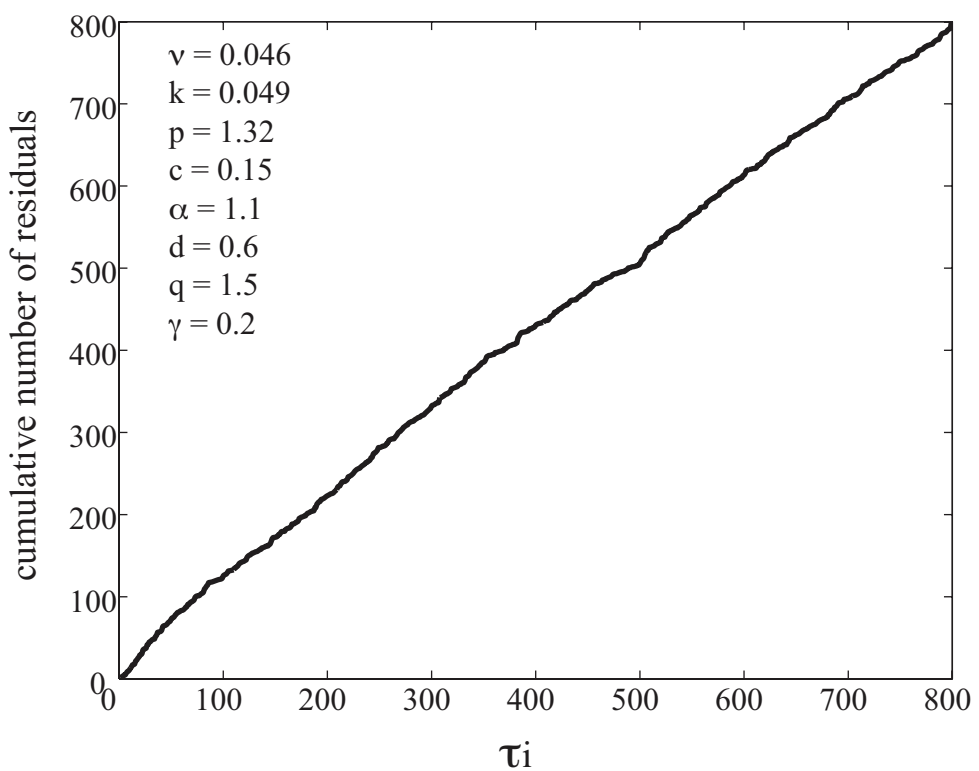


Figure 6

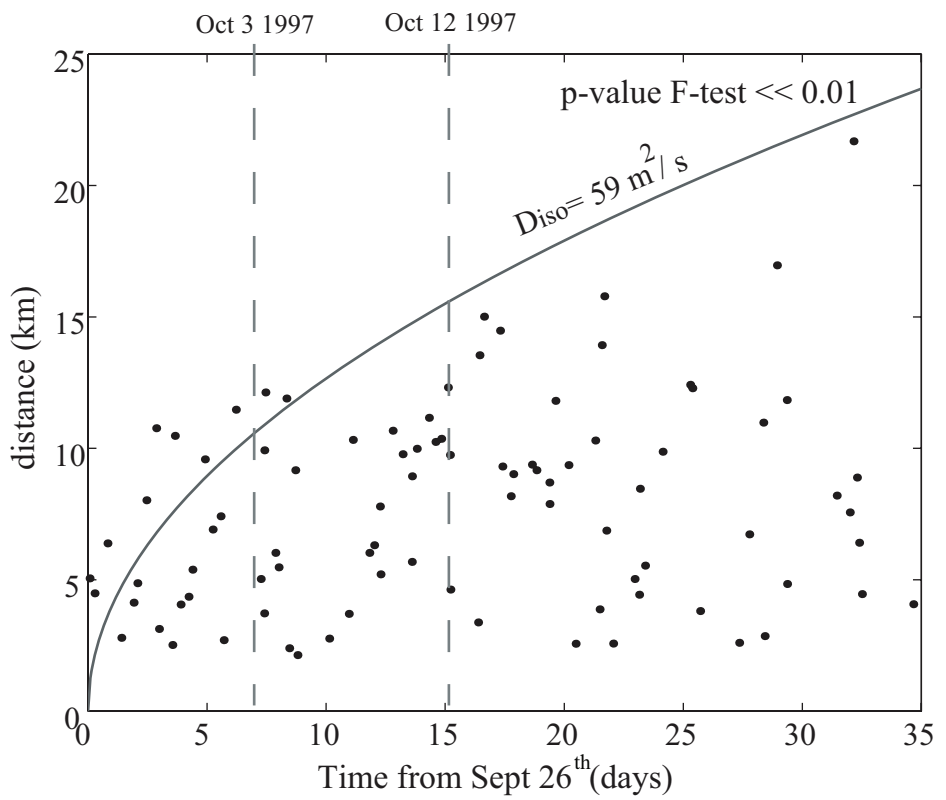


Figure 7

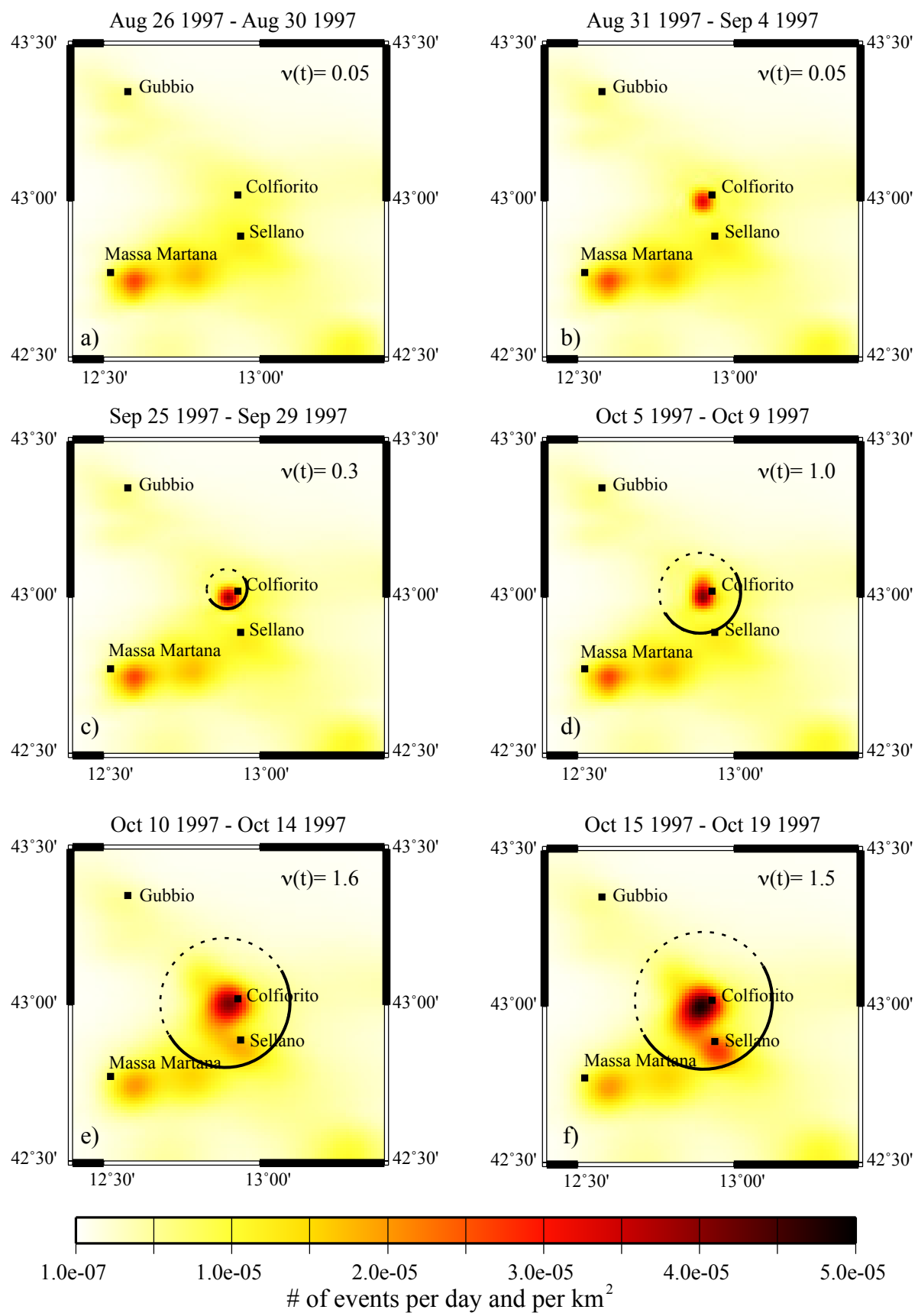


Figure 8